

# Sedimentary hydrodynamic study of sand bodies in the upper subsection of the 4th Member of the Paleogene Shahejie Formation in the eastern Dongying Depression, China

Jiang Zaixing<sup>1\*</sup>, Liang Shuyi<sup>1</sup>, Zhang Yuanfu<sup>1</sup>, Zhang Shanwen<sup>2</sup>, Qin Lanzhi<sup>3</sup> and Wei Xiaojie<sup>1</sup>

<sup>1</sup> School of Energy Resources, China University of Geosciences, Beijing 100083, China

<sup>2</sup> Shengli Oilfield Branch Corporation, SINOPEC, Dongying, Shandong 257060, China

<sup>3</sup> CNOOC China Limited–Shanghai, Shanghai 200030, China

© China University of Petroleum (Beijing) and Springer-Verlag Berlin Heidelberg 2014

**Abstract:** Petroleum is produced from a beach-bar sand reservoir in the upper subsection of the 4th member of the Paleogene Shahejie Formation ( $Es_4^s$ ) in the eastern Dongying Depression, penetrated by many wells in the Guangli-Qingnan area and this subsection still has further exploration potential. Using drilling and logging data, we analyzed the sand body types, emphasizing the sedimentary characteristics of the beach-bar sand bodies. Combining these data with the concepts of lacustrine and oceanic hydrodynamics, we explain the formation and distribution of the beach-bar sands in the eastern Dongying Depression. The connectivity between beach-bar sand bodies within each individual hydrodynamic zone is better than that between sand bodies in any two adjacent zones. The tempestite sand bodies developed in this area are characterized by typical storm deposits and are located at the bottoms of the beach-bar sand bodies. They grade upward to normal shore and shallow-lacustrine beaches and bars. We also propose a new simple method to estimate the paleo-water depth using the thicknesses of the bar sand bodies in parasequences combined with the principle of hydrodynamic zonation. Based on the distribution of the beach-bar sands in parasequence set 3, we infer that the paleo-wind direction was from the north with an average paleo-wind force of 6 when the major beach-bar sand bodies formed.

**Key words:** Beach-bar, sedimentary hydrodynamic zone, paleo-water depth, paleo-wind force

## 1 Introduction

Beach-bar sand bodies commonly develop along the shallow shore zones of lakes. The definition, classification, depositional models and identifying features of these bodies have been studied systematically by many scholars. Originally, Campbell (1971) and Fraser and Hester (1977) developed various beach-bar depositional models based on extensive field surveys. Thereafter, the importance of beach-bar sand bodies to hydrocarbon accumulations began to be recognized. Researchers, including Tesson et al (2000) and Graham (2000), analyzed the sedimentary characteristics of beach-bars by looking at examples. Others, including Zhang (1995), Zhu et al (1994), Chen et al (2000), Chang et al (2005), and Wu et al (1998), performed detailed studies and described the rock material composition, distribution, provenance and

hydrodynamic environment of the beach bars. The beach-bar facies were identified using the conventional methods of lithological characteristics, for example, texture, structure and well logging curves, and also using other special means. Researchers, including Tucker and Vacher (1980), developed a linear discriminant based on relevant matrix characteristics, including grain size distributions, to identify beach-bar sand bodies. Others, including Cai (2005) and Liu (2006), used seismic inversion to identify beach-bar sand bodies. Anfuso et al (1999), for example, used a depositional thickness chart of sand bodies to identify beach-bars. Although extensive studies of beach bars have been conducted by many scholars, the thinly bedded but widely distributed beach sand bodies and the thickly bedded but narrowly distributed bar sand bodies in fault basins cannot be definitively classified using the limited drilling and seismic data (Zhu et al, 1994; Chen et al, 2000; Yu et al, 2011). We propose that the beach sand bodies and the bar sand bodies can be distinguished by studying the sedimentary characteristics of beach bars in the

\*Corresponding author. email: jiangzx@cugb.edu.cn

Received March 14, 2013

Paleogene  $Es_4^s$  in the eastern Dongying Depression.

Beach bars are primarily formed by the actions of waves and lake currents. Waves are the predominant elements that control coastal hydrodynamics and the development of the coast (Levoy et al, 2013). In this article, we combined lake hydrodynamics with ocean hydrodynamics and used hydrodynamic zonation to explain the formation and distribution of beach bars of  $Es_4^s$  in the eastern Dongying Depression. The formation of waves is closely related to the lake wind force. The study of wind force is very important to explain the genesis of beach bars (Castelle et al, 2007; Li et al, 2013). The various beach-bar sand bodies formed in different hydrodynamic zones. The beach-bar sand bodies developed in various paleo-water depths associated with various hydrodynamic zones (Karambas and Koutitas, 2002). Using the observations of drill cores collected from 20 wells and analyses of composite logs of 80 wells, the paleo-water depth, paleo-wind force and paleo-wind direction of this area were estimated.

## 2 Geological setting

### 2.1 Regional geological setting

The study area is located in the eastern Dongying

Depression which includes the Niuzhuang sag and Wangjiagang fault-nose structure zone, and has an area of approximately 1,000 km<sup>2</sup>. The bedrock consists of a large horst, called the Chunhua buried hill, bounded by the Chenguanzhuang and Bamianhe faults. The ground surface in the study area generally slopes to the northwest. The area, therefore, has the aspect of a gentle horst zone. South of the area, there is a gentle slope that is close to the Guangrao salient, and to the northeast, there is a steep slope that is close to the Qingtuozi salient. The western part of the Dongying Depression is separated from the Boxing sag by the NW-trending Chunhua-Caoqiao fault-nose structure zone and it is separated from the Lijin sag by an EW-trending central fault anticlinal zone. The study area is divided into four second-order structural zones (Fig. 1), specifically the south slope of the Niuzhuang sag, the Chenguanzhuang-Wangjiagang fault anticlinal zone, the Bamianhe fault-nose structure zone and the north slope of the Guangrao salient (Wang et al, 2011).

### 2.2 Sequence stratigraphy

The Cenozoic strata, which are widely distributed in the eastern Dongying Depression, include, from bottom to top, the Quaternary Kongdian, Shahejie, Dongying, Guantao, Minghuazhen and Pingyuan Formations. Based on

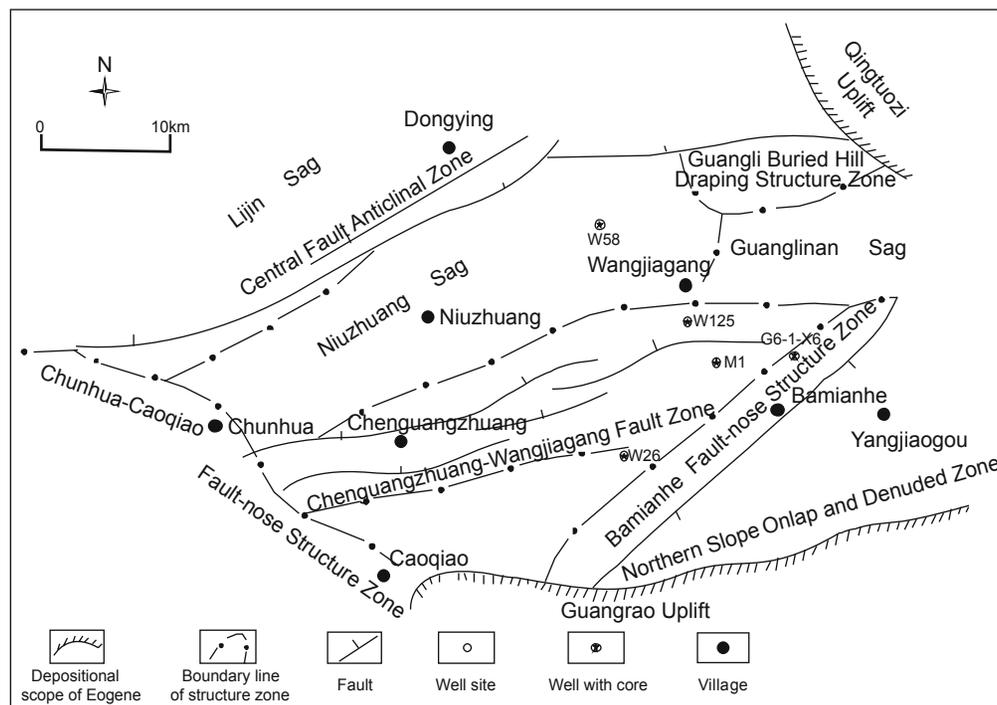


**Fig. 1** The secondary structural diagram of the eastern Dongying Depression

stratigraphic characteristics, the 4th member of the Shahejie Formation, which is designated member  $Es_4$ , can be divided into upper, middle, and lower submembers in this area. Its upper submember,  $Es_4^s$ , can be further divided into the upper-Chun subsection and the lower-Chun subsection, which is the major oil-bearing formation. In terms of lithology, the upper-Chun subsection of  $Es_4^s$  consists of dark gray and brown gray interbedded mudstone, oil shale, sandstone and limestone. Generally, the thickness of this layer is approximately 100

m, and the maximum thickness is 175 m. Under the influence of the slope, the strata thin toward the south. The resistivity log displays dagger shapes and abnormally high amplitudes. The lower-Chun subsection of  $Es_4^s$  consists of dark gray interbedded mudstone, oil shale, sandstone, limestone, and dolostone. The strata are laterally continuous and display average thicknesses of tens of meters. The resistivity log has the appearance of a comb with teeth and shows abnormally high amplitudes (Li et al, 2003; Li et al, 2008).

Based on classic sequence stratigraphy theory, submember Es<sub>4</sub><sup>s</sup> can be considered as a third-order sequence in this area (Jiang et al, 2011; Xu et al, 2013) (Fig. 2), and seismic reflection T<sub>7</sub> is the boundary between the lowstand systems

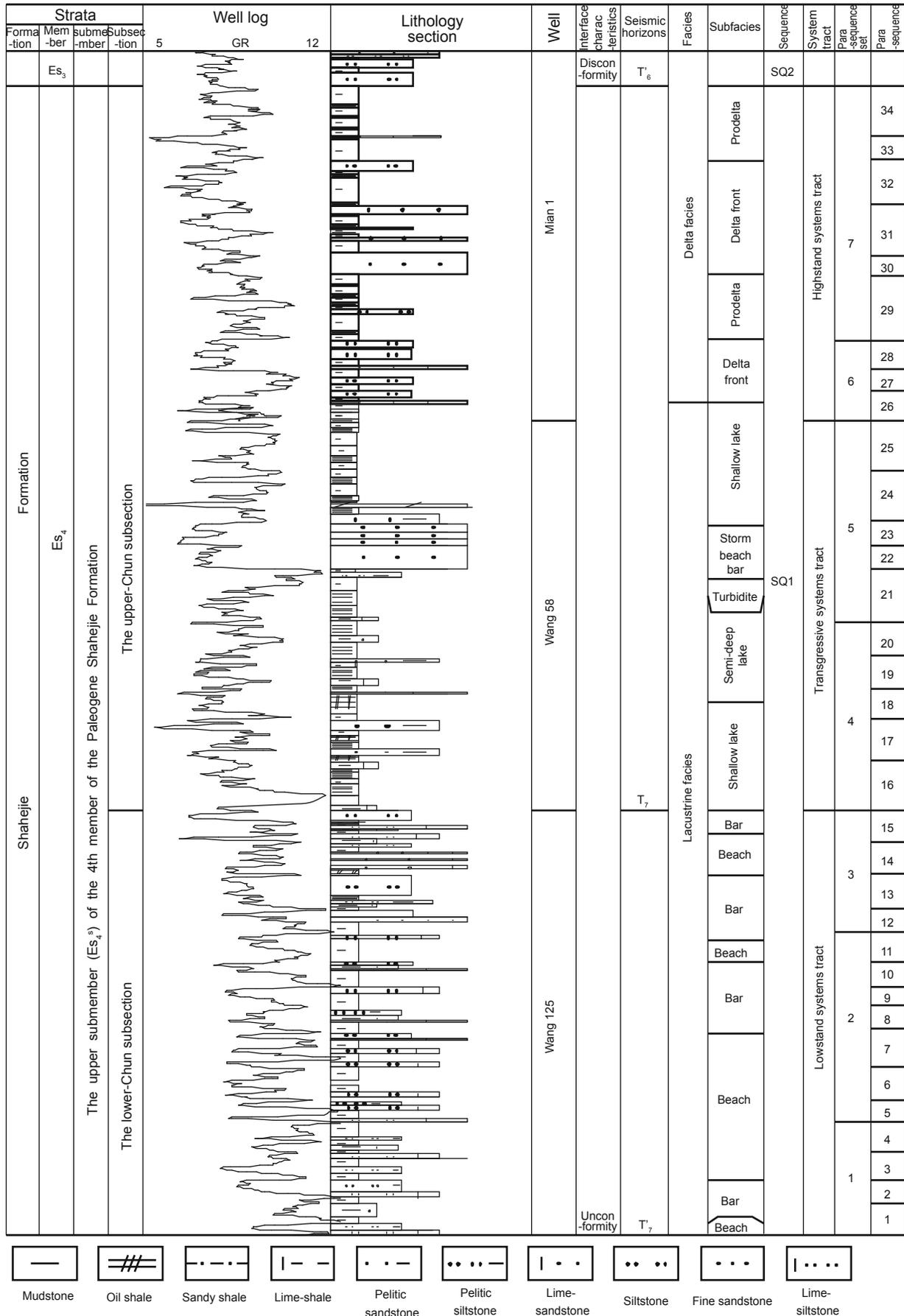


Fig. 2 Stratigraphic column of the Shahejie Formation, eastern Dongying Depression

tract (LST) and the transgressive systems tract (TST). The lower-Chun subsection is the LST and can be further divided into three progradational parasequence sets. The upper-Chun subsection consists of a TST and highstand system tract (HST), and the TST can be further divided into two retrogradational parasequence sets, whereas the HST is further divided into one progradational parasequence set and one aggradational parasequence set.

### 3 The type of sand body and sedimentary characteristics

In this study area, the sand bodies of submember Es<sub>4</sub><sup>s</sup> record the presence of primarily delta, shore and shallow-lacustrine beach-bar and storm beach-bar paleoenvironments.

#### 3.1 Delta front sand bodies

A minor sediment supply entered the basin from the eastern part of the area, and delta front sand bodies developed from a poor supply of sediments were deposited primarily in the southern part of the Guangli sag during the time of the TST and HST of Es<sub>4</sub><sup>s</sup>. The lithologies of the delta front include gray fine-medium sandstone, calcareous sandstone and siltstone. The sandstones display evidence of strong paleocurrents. In underwater distributary channels, sandstones primarily developed with thinly bedded mudstones, cross-bedding, trough cross-bedding and small ripple cross-bedding.

A positive fining upward sequence formed in a vertical section. At the bottom, a scoured surface developed over which clay boulder and fining upward sediments were deposited. The overlapping channel sand bodies are tens of meters thick. The mouth bars consist of well-sorted sandstone interbedded with gray mudstone, with low angle cross-bedding, parallel bedding and wave-ripple bedding. The lithology, from bottom to top, indicates that the sand bodies are composed of pelitic siltstone and silty fine sandstone. This series of sand bodies form a coarsening upward sequence. The thickness of any single sand body varies from 1 to 5 m. The shape of the SP curve is funnel-shape, and the lower part is a gradual contact; the shape of the apparent resistivity curve is serrated funnel-shape.

#### 3.2 Shore-shallow lacustrine beach-bar sand body

As submember Es<sub>4</sub><sup>s</sup> represents an open shore and shallow lake area, many beach-bar sand bodies developed in the gentle slope zone in the eastern and southern parts of the Dongying Depression (Zhang et al, 2006). Based on a paleogeographic analysis, those authors inferred that the Guangrao uplift, south of the research area, was the primary source area of the beach-bar sediments. Due to the absence of a large sediment supply on the Guangrao uplift at that time (Song et al, 2012), the small sediment supply was subject to only minor sorting along a short transport path and was subsequently deposited on the lake edge, where it was reworked by strong waves and longshore currents and formed a considerable beach-bar system.

Unlike the delta system, the beach-bar system was

characterized by a poor supply of sediment due to the shallow water conditions (Allen and Allen, 1990; Zhang et al, 2010). At the edge of the basin, waves and longshore currents were strong (Zeng et al, 2012), which, together with the meager sediment supply, resulted in the deposition of carbonate rocks. This is why carbonate rocks can usually be found in the sandy beach-bars. Moreover, the beach-bar sandstones were always cemented by carbonate and became calcareous sandstone.

On the basis of the shapes and positions of the sandstones, the beach-bar sandstone can be divided into two types: beach sand and bar sand. Bar sandstones, thick and coarse grained, were always distributed in topographically high positions, namely the hanging wall of the Bamianhe fault. In contrast, the beach sandstones are thin and finely graded and contain significant interbedded claystone (Jiang et al, 2011). We used the lithology, grain size, sedimentary structures and well logging data to distinguish the beach and bar sandstones in this area.

##### 3.2.1 Beach subfacies

**Lithology:** Beach lithology generally consists of sandstone interbedded with claystone. The sandstone layers are abundant but thinly bedded, and the thin interbedded claystone layers are primarily gray green and light gray mudstone (Fig. 3(a)). The sandstones are primarily well-sorted siltstone with a minor amount of fine sandstone and argillaceous siltstone. These layers always coarsening upward, although this feature may not be clear in places.

**Grain size:** The cumulative probability curve developed for the beach sand bodies exhibits a gentle slope and a multi-population pattern. The curve shows evidence of a rolling population, saltation population, including backflow and a washing out point, and a suspension population. The total gradient is relatively low. The grain size separating the rolling and saltation populations is in the range of 1 to 1.5  $\phi$ , and that separating the rolling and suspension populations is approximately 3.5  $\phi$ . The relationship of  $\phi$  and particle diameter is that:  $\phi = -\log_2 D$ ,  $D$ : particle diameter (mm).

**Structure:** Because this lithofacies was deposited near the shoreline, plant fragments are common in the beach sand bodies and carbon dust is distributed throughout the layers. Layers of intact plant fragments and shells are abundant because of the weak hydrodynamic conditions along the shoreline beach. The typical sedimentary structures in the beach sand bodies are swash cross-bedding, indicating bidirectional wave swashing conditions. The single sand strata are thin, and claystone interbeds are common. Lenticular bedding and composite wavy bedding are developed.

**Well logging data:** The shapes of the GR and SP curves from the beach sand bodies are mostly dagger-like fingers with abnormally high amplitudes, indicating a reverse cycle with an increasingly abnormal amplitude from the bottom to the top.

##### 3.2.2 Bar subfacies

**Lithology:** The bar profiles are characterized by thick sandstones interbedded with mudstones. The thickness of a single bar sand body can be several meters or more. The mudstones are primarily light gray and gray pure mudstone

and organic-rich shale (Fig. 3(b)). The sand body is primarily thick pure siltstone. The vertical sequences of grain size grading are complex, and reverse rhythm sequences are common. In profile, the sand bodies have a lenticular shape; these lenses are either biconvex or have a convex top and flat bottom.

**Grain size:** The cumulative probability curves developed for the bar sand body generally show two patterns. The first is a two-population pattern with a saltation population and a suspension population. The saltation portion of the curve has a steep slope, and the suspension population is substantial, up to thirty percents. The grain size point separating the saltation and suspension populations is approximately 3.5  $\phi$ . The

second pattern is a steeply sloping, multi-population pattern that includes a rolling population, saltation population (with a backwash-swash point) and suspension population, with a steeply sloping portion of the curve.

**Structure:** Compared to the beach sand bodies, fossils are rare in the bar sand bodies, while plant fragments and clam shell fragments are minor and burrows are abundant. Typical structures due to wave action, such as wave-ripple cross-bedding, wavy bedding, parallel bedding and wedge-shaped bedding, are developed.

**Well logging data:** The shapes of the GR and SP curves from the bar sand bodies are mostly broad finger or serrated funnel shapes, indicating a reverse cycle.

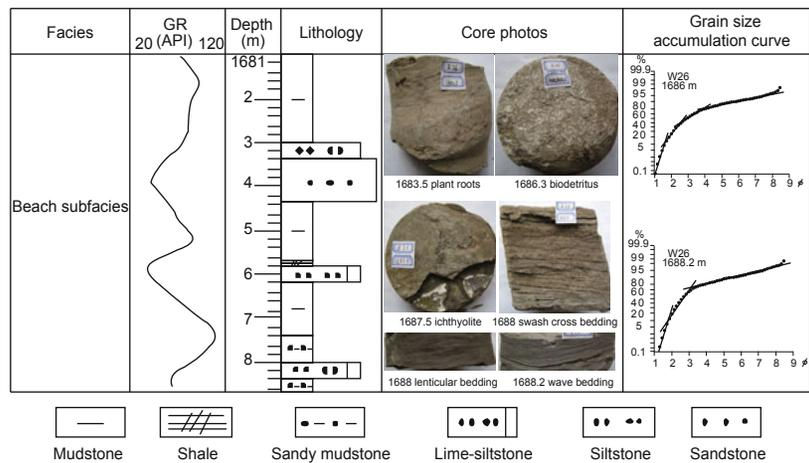


**Fig. 3 (a)** Features of beach subfacies sand body (well W26)

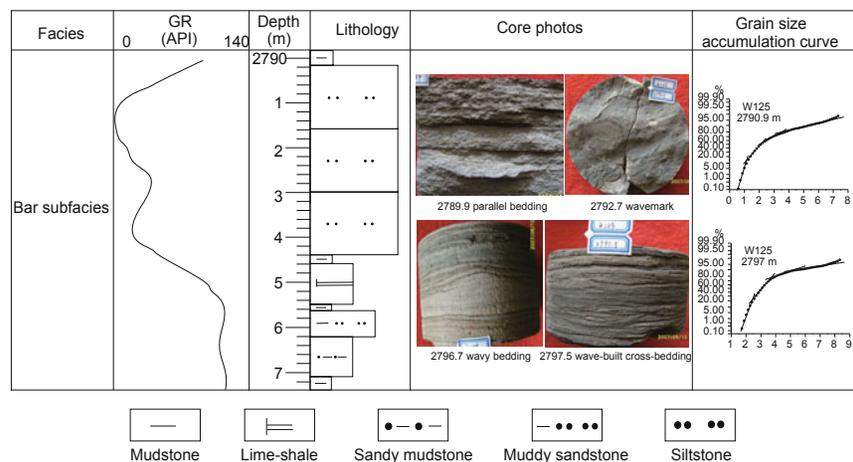


**Fig. 3 (b)** Features of bar subfacies sand body (well W125)

## 4 Sedimentary hydrodynamic characteristics

### 4.1 Sedimentary dynamic zones

#### 4.1.1 Fundamental principle

During the depositional period of the LST, beach-bar sand bodies developed along the lake coastline in the southern gentle slope zone with little sediment supply from the Guangrao Uplift. The hydrodynamic conditions were much

similar to those of the ocean. Wave and lacustrine currents were also present in lakes (Bohacs et al, 2000). From the lakeshore to the central lake, the lithology changed from coarse to fine due to the attenuation of the hydrodynamic intensity. The larger the lake, the more commonalities with the ocean can be found, especially the ocean's neritic zone, where tidal action is insignificant (Feng, 1993; Jiang, 2003). The characteristics of beach-bars in this study were primarily evaluated in terms of nearshore marine hydrodynamics.

The formation of the beach-bars was primarily controlled by lacustrine waves and longshore currents (Carroll and Bohacs, 2001). Because the water was quiet below the wave base, the sand bodies developed only rarely and were primarily distributed in a depth zone between the average lake surface level and the normal wave base. Tempestites are usually deposited in a depth zone between the storm wave base and the normal wave base. The wave characteristics and their influence on sediment transport and deposition varied between environments and depth zones of the lake (Feng, 1993; Jiang, 2003; Castelle et al, 2007). As the waves spread shoreward, they reached a point where the lake floor was at approximately the same depth as the wave base; farther shoreward, the wave grew taller as the water depth decreased. Where the waves reached a water depth twice the wave height, the waves became rolling and broken; this region is called the "breaker zone". The waves were very turbulent in this region, and they eroded the lake floor and selectively transported coarse fragments toward the lake shore. As a result, the grains were coarser along the beach-bars. In the study area, primarily fine sandstone and siltstone were deposited. Farther shoreward still, where the water depth was equal to the wave height, the wave crests were back rolling and broken completely, called "surf" or "swells", and this region is called the "surf zone" or "surge zone". The development and width of the surf zone are controlled by the topographic slope. Because the slope in the southern part of the study area was gentle, a broad surf zone developed and the grain sizes were finer than those in the breaker zone; primarily siltstone and pelitic siltstone were deposited in this area. After the surf and swells moved up onto the beach, the water rushed landward to produce a "wash zone" or "swash zone", which contained incoming waves that moved under inertia and rip currents that returned to the lake under the influence of gravity. Waves in the swash zone washed the sandy shores repeatedly, and the beach-bars consequently contained sediment with high compositional and textural maturity. In the study area, the beach-bar deposits are primarily composed of siltstone and pelitic siltstone. The color of the mudstone is primarily gray-green, green, and sometimes red. Beach-bars of the LST in the study area are primarily distributed within the breaker, surf and swash-backwash zones.

#### 4.1.2 Application

##### 1) Tempestite beach-bar

Lacustrine tempestites have been identified in modern sedimentary environments and in the rock record (Duke, 1985; Zhang et al, 1987; Sun and Wu, 1986). Beach-bars deposited by storm action between the storm wave base and the normal wave base are called tempestite beach-bars.

**Lithology:** The lithological profile of the tempestite beach-bars is characterized by conglomeratic fine sandstone at the bottom, grading upward into fine sandstone and siltstone. The size grading of these sediments, which display a positive rhythm cycle, is complex. The shapes of the sand bodies in the section are lenticular and are either biconvex or display convex tops and flat bottoms.

**Grain size:** Storm currents primarily contained traction

currents and may also exhibit certain characteristics of gravity flow, and the sediment grain size curves from the tempestite beach-bars are thus of many types. In the study area, the grain size curves primarily indicate traction current characteristics of the attenuating stage with low energy. Compared with gravity flow deposition, sediments deposited by storms in the lake displayed high textural maturity, a low percentage of matrix, and were moderately sorted. In addition, all of the grain size probability curves display clear patterns of multiple saltation populations and one suspension population. The percentage of grains in the suspension population is lower than that of turbidity current deposition. Tempestite beach-bars in the study area can be subdivided into the lateral margin and the primary body. According to the cumulative probability grain size curve from a sample from well W58, there are two saltation populations and one suspension population at the lateral margin. The steep slope of the curve indicates the influence of multicomponent currents and good sorting. The saltation population comprises between 60% and 70% of the material, and the grain size separating this population from the suspension population is approximately  $3.5 \phi$ . The grain size curve of the sample from the primary body displays evidence of two saltation populations and one suspension population. The curve shows the presence of multicomponent currents and good sorting. The saltation population comprises between 80% and 90% of the material, and the grain size that separates this population from the suspension population is approximately  $3.5 \phi$ . In addition, the curve slopes steeply.

**Sedimentary sequence:** The sequence of tempestite beach-bars in this area consists of three sedimentary units (Fig. 4). Unit A consists of a section of sandstone with hummocky or sunken cross-bedding and a section of fine sandstone with cross-bedding. This section consists of medium-coarse sandstone and exhibits a gently scoured surface at the bottom. Typical wedge-shaped clay boulder is present, and the sandstone displays hummocky cross-bedding and typical cross-bedding. Unit B consists of a section of fine sandstone with typical wavy bedding and a boulder clay with paleocurrent indicators in the top as the result of erosion by storm waves and buffeting. Unit C consists of a fine sandstone with wedge cross-bedding and a mudstone segment with horizontal bedding. The above-mentioned sequence indicates the normal sedimentary sequence of a beach-bar during the process of storm weakening and disappearance (Du and Han, 2000; Patranabis-Deb et al, 2007). After the storm, the lake deepened and normal waves did not rework the relict tempestite beach-bar, which assisted its preservation (Jiang et al, 1990; Gao et al, 1999; Yang et al, 2007).

**Well logging data:** In contrast to that of other (shallower) beach-bars, the shape of the gamma ray curve from the tempestite beach-bar looked like a bell. It displayed a positive rhythm cycle with fining upward.

##### 2) Beach-bar of the shore-shallow lacustrine deposition

We discuss parasequence 3 as an example that can be explained using the sedimentary hydrodynamic lake zone theory (Fig. 5). Based on the vertical superimposition features and horizontal distribution of the beach-bar sand bodies, we

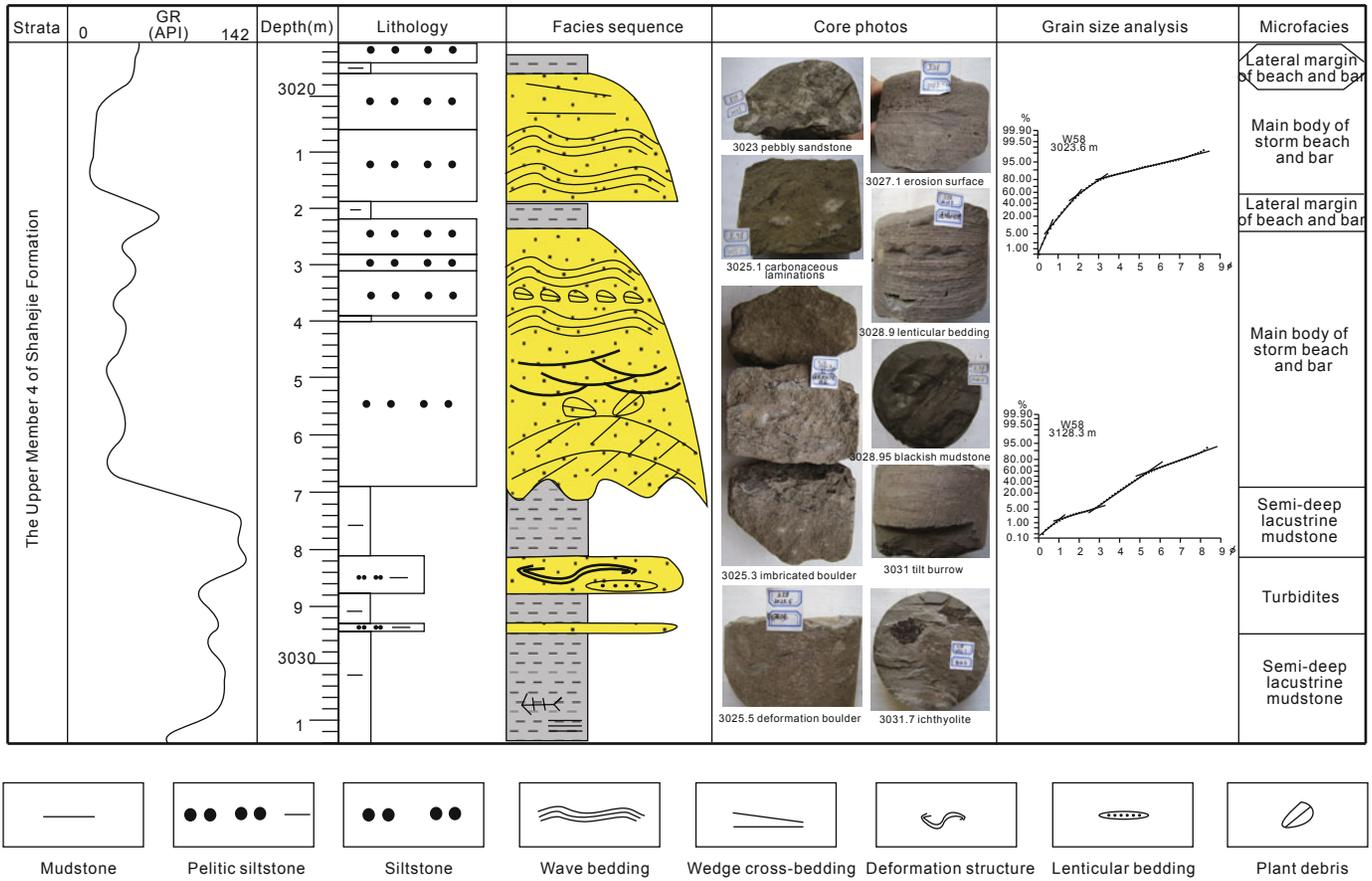


**Fig. 4** Sedimentary sequence of the tempestite beach-bar (well W58)

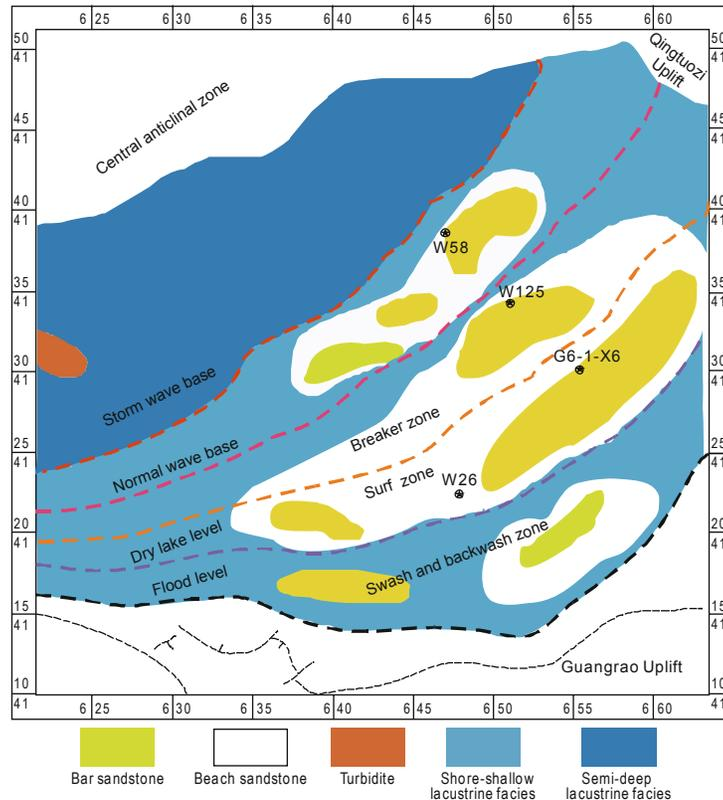


**Fig. 5** Sedimentary hydrodynamic zones and distribution of sand bodies

concluded that various beach-bars each formed under different hydrodynamic forces. Because of the strong hydrodynamic forces in the breaker zone, the grains of the sand bodies in this zone were coarse, and these fine sandstones generally developed with good connectivity. The hydrodynamic force in the surge zone was weaker, and silt layers with a fine grain size and good connectivity were generally deposited in this zone. However, the lateral connectivity between the sandstones of the surge and breaker zones was poor. Beach sand dominated the swash and backwash zones. The primary colors of the mudstone were red and green, indicating shallow water and that the sand bodies were distributed along the coastline. The lateral connectivity between beach-bar sand bodies within each sedimentary zone was generally good but was poor between any two adjacent zones.

## 4.2 Paleo-water depth

Determining the paleo-water depth is an important research topic in paleolimnology and has a great significance in studying the depositional environments and histories of the source, reservoir and cap rocks (Li et al, 2005). We can estimate the paleo-water depth of the lake basin on the basis of the distribution of sediments, sedimentary structures (Ji et al, 2005), paleontological evidence (Li et al, 2005; Gao et al, 2009; Zou and Ge, 2000), and ecology (Zhang and Ren, 2003), although the estimate of paleo-water depth is primarily qualitative and relative.

We used paleotopography and paleohydrodynamic conditions to construct a depositional model of the beach-

bars. Based on the definition of a beach-bar in this context, the sediment color, lithology, well logging curves and locations of sand bodies, we have identified various discrete beach-bars. The formation of a beach-bar indicates a change in the paleo-water depth. Accordingly, we propose a new method for estimating the paleo-water depth using the thicknesses of the bar sand bodies.

### 4.2.1 Principle

Based on the principle that different hydrodynamic zones form different types of beach-bars, especially regarding their distribution and thicknesses, we thought that each bar sand body's thickness was equal to the paleo-water depth above the normal wave base under conditions of adequate supply of detritus at that time. This relationship means that the thickness of one parasequence during the formation of the bar was equivalent to the paleo-water depth (Fig. 6). The top of the coastal bar was below the flood-level lake surface, while the top of the distal bar was the same as the bottom of the coastal bar, as determined by the bar characteristics. Consequently, we can estimate the paleo-water depth, as long as we calculate the thicknesses of the individual bar sand bodies. As shown in Fig. 6, the thickness of the coastal bar was  $H_3$ ; this was also the paleo-water depth. The paleo-water depth of the nearshore bar was the sum of the height of the coastal bar and nearshore bar, equal to  $H_3+H_2$ , and the paleo-water depth of the distal bar was the sum of  $H_3$ ,  $H_2$  and  $H_1$ . Therefore, the paleo-water depth of the tempestite beach-bar was the sum of the height of the bar sand bodies above the storm wave base and was equal to the sum of  $H_3$ ,  $H_2$ ,  $H_1$  and  $H_0$ .

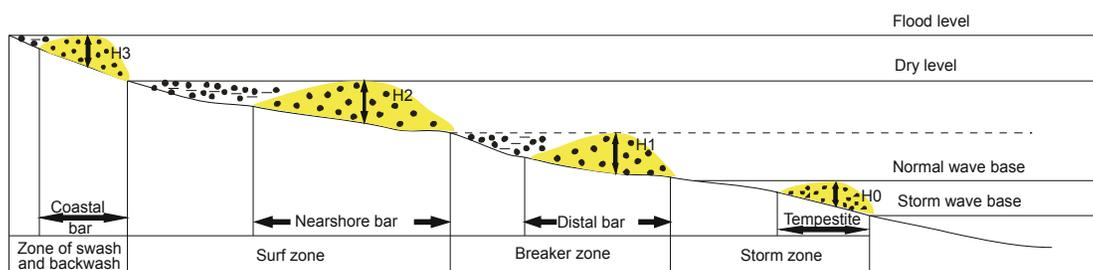


**Fig. 6** Calculation of paleo-water depth using the thicknesses of bar sand bodies

### 4.2.2 Application

There are many cores from wells in this area. We used a well section containing the whole facies sequence from the distal bar to the nearshore bar to indicate the paleo-water depth. Well G6-1-X6 is located in the Bamianhe Oilfield and was used as an example. By observing and analyzing the core, we find that a shore shallow-lacustrine beach-bar developed at this location (Fig. 7). Primarily fine sandstone and siltstone formed, and the color became lighter upward. Semi-deep lake mudstone and a tempestite bar, distal bar and nearshore bar developed, listed from bottom to top. No coastal bar appears in the drill core. According to the characteristics of bar sand bodies in the study area, the thickness of a single coastal bar was approximately 2 m. The thickness of the nearshore bar was 3 m and that of the distal bar was 2 m in the well. The water depth in each zone was estimated in

accordance with the foregoing theory and included additional adjustments to take into account structural compaction (Guo, 1998; Li et al, 2010). Consequently, the water depth of the zone of swash and backwash was between 0 and 2 m before adjusting for compaction and in the range of 0 to 4.5 m after adjustment. Similarly, the water depth in the surge zone was between 2 and 5 m before adjustment and in the range of 4.5 to 12.5 m after adjustment. In the breaker zone, the water depth was between 5 and 7 m before adjustment and in the range of 12.5 to 17 m after adjustment. The normal wave base was at a depth of 17 m, and the storm wave base was at a depth of 21 m. Earlier researchers using paleoecology and paleoenvironment analyses believed that the average water depth in the shore to shallow lacustrine or delta front zones was approximately 10 m, and the average water depth in the semi-deep and deep lake was approximately 30 m (Jiang et

al, 2009). The paleo-water depth estimated in our study is in the above range, which indicates that we can estimate the paleo-water depth of the lake by measuring the thicknesses of the bar sandstones.

The beach-bar sand bodies in the region primarily

developed on the southern slope during the LST. The paleo-water depth at various times and based on cores from wells can be estimated based on sedimentary facies analysis of a single well using the theory that paleo-water depth can be determined using the thicknesses of bar sand bodies.

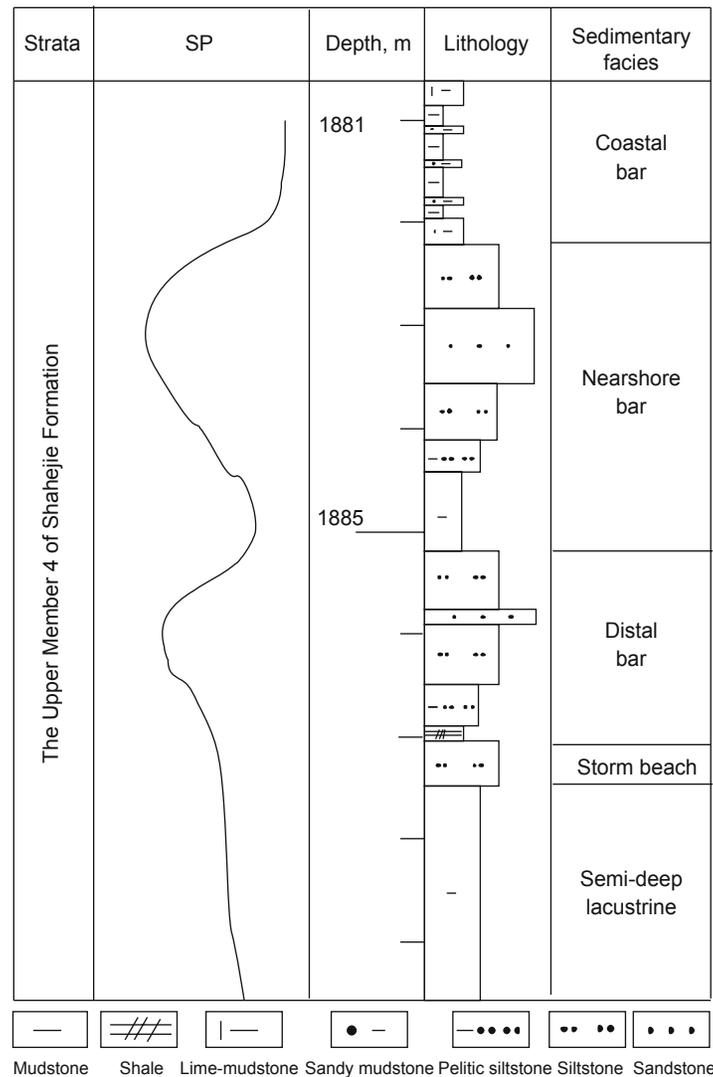


Fig. 7 Facies analysis of well G6-1-X6

4.3 Paleo-wind force

4.3.1 Concept

The formation of beach-bars is primarily influenced by waves and littoral currents. The wave intensity is controlled by the wind force. Therefore, estimating the wind velocity is significant for beach-bar research.

One of the key points in estimating wind velocity is the selection of the formula. Various formula are used for this purpose, most of which have been verified by a set of observed data; however, these formula use different data and are adapted to specific geographic conditions. According to the regional structural characteristics and the distribution of features of the beach-bars in the study area, we selected a calculation method for winds and waves as follows (Yang,

1996; Lin and Fang, 2012; Rao et al, 2012). According to the relationship of wind velocity and wind force, we can determine the wind force required to form a beach-bar.

$$gH / V^2 = 0.26th[0.587(gd / V^2)^{0.75}]th \{0.01(gF / V^2)^{0.5} / th[0.587(gd / V^2)^{0.75}]\}$$

where *H* stands for the average wave height (m); *F* stands for length of the area (km); *V* stands for the wind velocity (m/s); *d* stands for the water depth (m); and *g* stands for gravitational acceleration (m/s<sup>2</sup>).

4.3.2 Application

The beach-bar sand bodies developed during deposition of parasequence set 3 in the study area were taken as an

example. According to the formation and distribution of the beach-bars, we presumed that during this time the paleo-wind direction was primarily from the north. Based on our findings regarding the paleo-water depth, we estimated the wind velocity and wind force that had an important influence on the formation of the beach-bars using the method proposed above. The paleo-water depth was 17 m, based on the bar heights, as explained earlier. The wave height was 0.5 m, which was estimated based on the relationship between water depth and heights of the beach-bar sand bodies in the hydrodynamic zone. The fetch was 28 km, equal to the width of the lake; and the wavelength was 34 m. According to the calculation, we conclude that in the period when the beach-bars formed, the average wind velocity was approximately 12 m/s, or 6 on the wind force scale.

## 5 Conclusions

1) According to the analyses of sedimentary characteristics of the Es<sub>4</sub><sup>s</sup>, east Dongying Depression, we propose that delta front and beach-bar sand bodies developed in the study area.

2) According to sedimentological theory, we can distinguish the beaches and bars based on such features as their lithology, grain size, sedimentary structures, and well logging data. The beach sand bodies are characterized by thin interbedded sandstone and mudstone, with swash bedding, carbon dusts in the layers, and GR curves displaying dagger shapes. In contrast, the bar sand bodies are characterized by thick interbedded sandstone and mudstone containing wave-generated cross-bedding and parallel bedding, fewer paleontological fossils, and GR curves displaying broad finger shapes or serrated funnel shapes.

3) Based on the lake (and analogous ocean) hydrodynamic characteristics and the distribution of the beach-bars, we analyzed the formation of beach-bars in various hydrodynamic zones. We propose that the lateral connectivity between the beach-bar sand bodies within individual hydrodynamic zones was good, whereas it was poor between any two adjacent zones. We also found that tempestite beach-bar sand bodies had developed at the bottoms of beach-bar sand bodies in this area. These tempestite bodies were characterized by typical storm deposits, with the upper parts gradually grading into normal shore and shallow-lacustrine beach-bars.

4) We propose a new method to estimate the paleo-water depth using the thicknesses of bar sand bodies in parasequences and combine these with the principle of hydrodynamic zonation. The paleo-water depth estimated by the new method is close to that estimated by paleontological methods, and the method was simple.

5) Based on hydrodynamics, paleo-water depth, wave height, and fetch length and using the modern oceanographic method of estimating wind force based on wind velocity, we estimated the paleo-wind force when the beach-bar sand bodies formed. According to the distribution of beach-bars in parasequence 3, we deduce that the paleowind direction was from the north and the average paleowind force rated 6 on the wind force scale at that time.

## Acknowledgements

This study is supported by the National Major Research Program for Science and Technology of China (Grant No. 2011ZX05009-02), National Natural Science Foundation of China (No. 41102089). We are grateful to the Academy of Geosciences, Shengli Oil Field Branch Corporation for permitting data access.

## References

- Allen P A and Allen J R. Basin Analysis: Principles and Application. London: Blackwell Scientific Publications. 1990
- Anfuso G, Andres J, Vindel B, et al. Morphometric characteristics and internal structures of intertidal bars on the northwest Cadiz littoral (southwestern Iberian Peninsula). *Bol. Inst. Esp. Oceanogr.* 1999. 15(1-4): 203-211
- Bohacs K M, Carroll A R, Neal J E, et al. Lake-basin type, source potential, and hydrocarbon character: an integrated sequence-stratigraphic-geochemical framework. *AAPG Studies in Geology.* 2000. 46: 3-34
- Cai J H. Comprehensive application of technology with wave form analysis and seismic characteristic inversion to beach bar sandstones prediction—taking the area of Liang 108 in Boxing subsag as an example. *Oil & Gas Recovery Technology.* 2005. 12(3): 42-44 (in Chinese)
- Campbell C V. Depositional model—Upper Cretaceous Gallup beach shoreline, Ship Rock area, northwestern New Mexico. *Journal of Sedimentary Petrology.* 1971. 41(2): 395-409
- Carroll A R and Bohacs K M. Lake type controls on petroleum source rock potential in nonmarine basins. *AAPG Bulletin.* 2001. 85(6): 1033-1053
- Castelle B, Bonneton P, Dupuis H, et al. Double bar beach dynamics on the high-energy meso-macrotidal French Aquitanian Coast: a review. *Marine Geology.* 2007. 245(1-4): 141-159
- Chang D S, Lu G C, Kong F D, et al. Analysis on exploration of lake shallow-water beach and bar oil and gas reservoirs in Dagang exploration area. *China Petroleum Exploration.* 2005. 27(2): 26-32 (in Chinese)
- Chen S Y, Yang J P and Cao Y C. Sedimentary characteristics of two kinds of beach-bars of Oligocene Shahejie Formation in western Huimin Depression, China. *Coal Geology & Exploration.* 2000. 28(3): 1-4 (in Chinese)
- Duke W L. Hummocky cross-stratification, tropical hurricanes, and intense winter storms. *Sedimentology.* 1985. 32: 167-194
- Du Y S and Han X. Clastic tempestite and its significance in Yinmin Formation, Kunyang Group (Mesoproterozoic) in Central Yunnan Province. *Acta Sedimentologica Sinica.* 2000. 18(2): 259-261 (in Chinese)
- Feng Z Z. *Sedimentary Petrology.* Beijing: Petroleum Industry Press. 1993. 123-126 (in Chinese)
- Fraser G S and Hester N C. Sediments and sedimentary structures of a beach-ridge complex, southwestern shore of Lake Michigan. *Journal of Sedimentary Research.* 1977. 47(3): 1187-1200
- Gao S L, Chen H H, Dou W T, et al. Lacustrine storm sediment in Yanchang Formation of Ordos Basin. *Acta Sedimentologica Sinica.* 1999. 17(supplement): 758-761 (in Chinese)
- Gao Z Y, Guo H L, Zhu R K, et al. Sedimentary response of different fan types to the Paleogene-Neogene basin transformation in the Kuqa Depression, Tarim Basin, Xinjiang Province. *Acta Geologica Sinica (English Edition).* 2009. 83(2): 836-846
- Graham J P. Revised stratigraphy, depositional systems, and hydrocarbon exploration potential for the Lower Cretaceous muddy sandstone,

- northern Denver Basin. *AAPG Bulletin*. 2000. 84(2): 183-209
- Guo Q L. *Basin Modeling Rule and Approach*. Beijing: Petroleum Industry Press. 1998. 8-15 (in Chinese)
- Jiang D Y, Motani R, Hao W C, et al. Biodiversity and sequence of the Middle Triassic Panxian marine reptile fauna, Guizhou Province, China. *Acta Geologica Sinica (English Edition)*. 2009. 83(3): 451-459
- Jiang Z X. *Sedimentology*. Beijing: Petroleum Industry Press. 2003. 330-331 (in Chinese)
- Jiang Z X, Liu H, Zhang S W, et al. Sedimentary characteristics of large-scale lacustrine beach-bars and their formation in the Eocene Boxing Sag of Bohai Bay Basin, East China. *Sedimentology*. 2011. 58(5): 1087-1112
- Jiang Z X, Zhao C L and Yuan Z W. Preliminary study of lake facies storm deposits in the west Dongpu Sag. *Acta Sedimentologica Sinica*. 1990. 8(2): 107-113 (in Chinese)
- Ji Y L, Feng J H, Wang S L, et al. Shifting of lake shoreline and lithofacies palaeogeographic characters during sedimentary period of the Member 3 of Shahejie Formation of Paleogene in Dongpu Sag. *Journal of Palaeogeography*. 2005. 7(2): 145-156 (in Chinese)
- Karambas T V and Koutitas C. Surf and swash zone morphology evolution induced by nonlinear waves. *Journal of Waterway, Port, Coastal, and Ocean Engineering*. 2002. 128(3): 102-113
- Levoy F, Anthony E J, Monfort O, et al. Formation and migration of transverse bars along a tidal sandy coast deduced from multi-temporal Lidar datasets. *Marine Geology*. 2013. 342(1): 39-52
- Li G B, Jiang Z X, Wang S L, et al. The quantitative prognosis of thin interbedded beach-bar sandbodies: a case study of the upper 4th submember of the Paleogene Shahejie Formation in Dongying Sag. *Geology in China*. 2010. 37(6): 1000-3657 (in Chinese)
- Li P L, Jin Z J, Zhang S W, et al. The present research status and progress of petroleum exploration in the Jiyang Depression. *Petroleum Exploration and Development*. 2003. 30(3): 1-4 (in Chinese)
- Li S J, Zheng D S, Jiang Z X, et al. Water depth of palaeo-lacustrine basin recovered by dominance diversity of Ostracoda: An example from sedimentary period of the member of Shahejie Formation of Paleogene in Dongying Sag, Shandong Province. *Journal of Palaeogeography*. 2005. 7(3): 399-404 (in Chinese)
- Li S M, Liu K Y, Pang X Q, et al. Quantitative prediction of mixed-source crude oils and its significance for understanding oil accumulation in subtle pools in the Dongying Depression, Bohai Bay Basin. *Petroleum Science*. 2008. 5(3): 203-211
- Li W H, Zhang Z H, Li Y C, et al. The main controlling factors and developmental models of Oligocene source rocks in the Qiongdongnan Basin, northern South China Sea. *Petroleum Science*. 2013. 10(2): 161-170
- Lin Y H and Fang M C. The assessment of ocean wave energy along the coasts of Taiwan. *China Ocean Engineering*. 2012. 26(3): 413-430
- Liu S H. Problems in thin-layer attribute analysis and solved methods—a case study in beach bar sandstones in Liang108 area of Dongying Sag. *Petroleum Geology and Recovery Efficiency*. 2006. 13(2): 56-58 (in Chinese)
- Patranabis-Deb S, Bickford M E, Hill B, et al. SHRIMP ages of zircon in the uppermost tuff in Chattisgarh Basin in central India require ~ 500-Ma adjustment in Indian Proterozoic stratigraphy. *Journal of Geology*. 2007. 115(4): 407-416
- Rao Y H, Liang S X and Yu Y X. A method to determine the incident wave boundary conditions and its application. *China Ocean Engineering*. 2012. 26(2): 205-216
- Song G Q, Wang Y Z, Lu D, et al. Controlling factors of carbonate rock beach and bar development in lacustrine facies in the Chunxia submember of Member 4 of Shahejie Formation in south slope of Dongying Sag, Shandong Province. *Journal of Palaeogeography*. 2012. 14(5): 565-570 (in Chinese)
- Sun S C and Wu Y F. Current sedimentation features of storm flow in Tai lake. *Chinese Science Bulletin*. 1986. 15(7): 537-541 (in Chinese)
- Tesson M, Posamentier H W and Gensous B. Stratigraphic organization of late Pleistocene deposits of the western part of the Golfe du Lion Shelf (Languedoc shelf), western Mediterranean Sea, using high-resolution seismic and core data. *AAPG Bulletin*. 2000. 84(1): 119-150
- Tucker R W and Vacher H L. Effectiveness of discriminating beach, dune, and river sands by moments and the cumulative weight percentages. *Journal of Sedimentary Research*. 1980. 50(1): 165-172
- Wang Y Z, Song G Q, Wang X Z, et al. Controlling effect of paleogeomorphology on deposition of beach and bar sand reservoir—case study of south slope, east Dongying Depression. *Petroleum Geology and Recovery Efficiency*. 2011. 18(4): 13-16 (in Chinese)
- Wu J H, Zhang Z and Wang B X. Barrier-lagoon sedimentary system and sequence development control of Shahejie Formation Member 1 of Dongying Sag. *Earth Science—Journal of China University of Geosciences*. 1998. 23(1): 21-25 (in Chinese)
- Xu J L, Liu L F, Wang G W, et al. Study of sedimentary sequence cycles by well-seismic calibration. *Petroleum Science*. 2013. 10(1): 65-72
- Yang B Z, Yang K G and Xia W C. Discovery of Middle-Upper Cambrian tempestites and its significance in Huangshi, Eastern Hubei Province. *Geological Science and Technology Information*. 2007. 26(3): 33-36 (in Chinese)
- Yang H. Wind wave computational method of fetch limited. *Electric Power Survey*. 1996. 12(4): 55-58 (in Chinese)
- Yu Y X, Chen D X, Pang H, et al. Control of facies and fluid potential on hydrocarbon accumulation and prediction of favorable Silurian targets in the Tazhong Uplift, Tarim Basin, China. *Petroleum Science*. 2011. 8(1): 24-33
- Zeng J H, Guo K, Tian K, et al. Hydrodynamic evolution and hydrocarbon accumulation in the Dabashan foreland thrust belt, China. *Acta Geologica Sinica (English Edition)*. 2012. 86(4): 912-923
- Zhang G D, Wang Y Y, Zhu J C, et al. Current shoreland storm deposit—Putuo Island in Zhoushan, Zhujiajian Island. *Acta Sedimentologica Sinica*. 1987. 5(2): 17-28 (in Chinese)
- Zhang J L. Beach and bar deposits of the Palaeogene Dongying formation in the Hejian oil field. *Scientia Geologica Sinica*. 1995. 4(4): 497-504
- Zhang S Q and Ren Y G. The study of base level changes of the Songliao Basin in Mesozoic. *Journal of Xi'an Engineering University*. 2003. 25(2): 1-5 (in Chinese)
- Zhang S W, Cioppa M T, Zhang S H, et al. Spatial variations in particle size and magnetite concentration on Cedar Beach: Implications for grain-sorting processes, Western Lake Erie, Canada. *Acta Geologica Sinica (English Edition)*. 2010. 84(6): 1520-1532
- Zhang Y W, Deng H W, Gao X, et al. High-resolution sequence stratigraphy and sedimentary facies evolution of the upper submember of the 4th member of the Shahejie Formation on the southern slope of the Dongying Depression, Shandong. *Sedimentary Geology and Tethyan Geology*. 2006. 26(3): 37-44 (in Chinese)
- Zhu X M, Xin Q L and Zhang J R. Sedimentary characteristics and models of the beach-bar reservoirs in down-faulted lacustrine basins. *Acta Sedimentologica Sinica*. 1994. 12(2): 20-28 (in Chinese)
- Zou X Q and Ge C D. The coccolith method for the quantitative study of former water depth—submarine sand ridges of the Yellow Sea as an example. *Geoscience*. 2000. 14(3): 263-266 (in Chinese)